mathematics

MDPI

Article

Fractional-Order MFAC with Application to DC Motor Speed Control System

Haizhen Wang [1], Huihua Jian [1], Jianhua Huang [2,3,*] and Yonghong Lan [4,*]

[1] School of Mechanical and Electrical Engineering, Xinyu University, Xinyu 338004, China; jhhxyxy@163.com (H.J.)
[2] Jiangxi Provincial Key Laboratory of Power Batteries and Energy Storage Materials, Xinyu University, Xinyu 338004, China
[3] Hunan Engineering Laboratory for Control and Optimization of PV Systems, Hunan Vocational Institute of Technology, Xiangtan 411104, China
[4] School of Automation and Electronic Information, Xiangtan University, Xiangtan 411105, China
* Correspondence: wxws1111@163.com (J.H.); yhlan@xtu.edu.cn (Y.L.)

Abstract: Model-free adaptive control (MFAC) can carry out various tasks using only I/O data, providing advantages such as lower operational costs, higher scalability and easier implementation. However, the robustness of MFAC remains an open problem. In this paper, a robust fractional-order model-free adaptive control (RFOMFAC) scheme is proposed to address the robust tracking control issue for a class of uncertain discrete-time nonlinear systems with bounded measurement disturbance. First, we use a fractional-order dynamic data model relating the relationship between the output signal and the fractional-order input variables based on the compact form dynamic linearization. Then, the pseudo-partial derivative (PPD) is obtained using a higher-order estimation algorithm that includes more information about past input and output data. With the introduction of a reference equation, a fractional-order model-free adaptive control (FOMFAC) law is then proposed. Consequently, using a higher-order PPD-based FOMFAC law can improve the control performance. Furthermore, a modified RFOMFAC algorithm with decreasing gain is constructed. Theoretical analysis indicates that the proposed algorithm can effectively attenuate measurement disturbances. Finally, simulation results demonstrate the effectiveness of the proposed method.

Keywords: model-free adaptive control; fractional order; robust; discrete-time system

MSC: 93D21

check for updates

Academic Editor: Ricardo Lopez-Ruiz

Received: 26 December 2024
Revised: 15 January 2025
Accepted: 25 January 2025
Published: 13 February 2025

Citation: Wang, H.; Jian, H.; Huang, J.; Lan, Y. Fractional-Order MFAC with Application to DC Motor Speed Control System. *Mathematics* **2025**, *13*, 610. https://doi.org/10.3390/math13040610

Copyright: © 2025 by the authors. Licensee MDPI, Basel, Switzerland. This article is an open access article distributed under the terms and conditions of the Creative Commons Attribution (CC BY) license (https://creativecommons.org/licenses/by/4.0/).

1. Introduction

Model-free adaptive control (MFAC) and data-driven control approaches focus on designing controllers using only the input/output data of the controlled system. These methods do not require the specific dynamic characteristics of the control system [1]. Thanks to its fewer identification parameters and wide range of application background, MFAC plays an important role in many fields and applications [2–4].

Using a concept called the pseudo-partial derivative (PPD), a series of equivalent dynamical linearized time-varying models are built along the dynamic operation points of the controlled plant. Generally, the dynamic linearization method includes three main forms: compact form dynamic linearization (CFDL), partial form dynamic linearization (PFDL), and full form dynamic linearization (FFDL). Using the CFDL technique, the MFAC-based consensus tracking scheme for multi-agent systems was proposed in [5]. Considering

the PFDL technique in case of multiple-variable systems, an improved model-free adaptive predictive control approach with application to vibration reduction of an elastic crane was developed in [6]. In [7], FFDL-based MFAC was investigated in a specific moving-mass controlled flying robot system. A high-order estimation algorithm was designed in [8,9] to estimate the value of PPD. An improved high-order MFAC method was proposed in [10], which considers more control knowledge from the previous time and uses more information from the previous time in the estimation algorithm.

Fractional-order MFAC (FOMFAC) is an attractive technique that has gained considerable interest in recent years. In [11], an FOMFAC algorithm was proposed based on the obtained fractional-order data-driven equivalent model. In [12], the inherent memory properties of fractional-order operators were considered in producing a discrete-time equivalent input–output data model, and the fractional PPD was computed to emulate networks by means of fuzzy rules. An event-triggered model-free adaptive fractional-order sliding mode controller was designed in [13]. In [14], the authors designed a fractional-order data-driven sliding mode controller for nonlinear systems. All parameters in the proposed controller were optimized using an artificial neural network.

Input/output data may suffer from external disturbances [15] or data dropout. Hence, it is interesting to investigate the robust performance of the MFAC algorithm. In [16], the authors presented a robust MFAC algorithm for a class of unknown MIMO systems with measurement noise. An adaptive decreasing factor was introduced to attenuate the effect of noise on performance, resulting in improved robustness of the algorithm. In [17], a data-driven MFAC law was designed for a mobile manipulator, with a radial basis function neural network (RBFNN) applied to approximate uncertainties in the data model. The problem of MFAC for the class of non-affine nonlinear systems with fading measurements was investigated in [18]. In [19], a data-driven control algorithm was presented by coupling MFAC and sliding mode control, with the aim of strengthening standard techniques in the presence of a class of output-dependent perturbations. An event-triggered MFAC problem for nonlinear networked control systems with presence of sensor faults and denial-of-service attacks was investigated in [2]. PID-like MFAC with discrete extended state observer was proposed in [20], with the external disturbance being rebuilt in order to reduce the influence of disturbance on PPD.

These observations motivate our current study. We present a novel MFAC approach. The main contributions of this paper mainly include two aspects:

1. Based on the CFDL technique, we use a fractional-order data-driven equivalent model and a high-order algorithm for PPD estimation to indirectly take advantage of more input and output data.
2. We propose a modified robust FOMFAC algorithm with variable gain, with the aim of attenuating the measurement disturbance.

The rest of this paper is organized as follows: some preliminaries and problem formulation are presented in Section 2; the robust FOMFAC algorithm and theoretical analysis are derived in Section 3; Section 4 provides numerical simulations to illustrate the validity of the design method; finally, our conclusions are drawn in Section 5.

Throughout this paper, $\mathbb{R}$ denotes the real number space, $\mathbb{N}$ represents the set of non-negative integers, and $\mathbb{N}^+$ means the set of positive integers.

2. System Description

Consider the following SISO discrete-time nonlinear system:

$$y(k+1) = f(k, y(k), \ldots, y(k-n_y), u(k), \ldots, u(k-n_u)) \tag{1}$$

where $u(k) \in \mathbb{R}$ is the control input, $y(k) \in \mathbb{R}$ is the system output at time instant k, and $n_y, n_u \in \mathbb{N}$ are two unknown integers.

Definition 1 ([11]). *The fractional-order difference operator for $u(k)$ is defined as*

$$\Delta^a u(k) = \sum_{i=0}^{\min(k,N)} w(i,a)u(k-i), \tag{2}$$

where $a \in (0,1)$ is the fractional order, $N \in \mathbb{N}$ is the buffer size, and

$$w(i,a) = \Big(1 - \frac{1+a}{i}\Big)w(i-1,a), \tag{3}$$

with $w(0,a) = 1$ as the fractional binomial coefficient.

Remark 1. *It can be seen that when $a = 0$, $\Delta u^0(k) = u(k)$, while when $a = 1$, $\Delta u^1(k) = u(k) - u(k-1)$ degenerates to the conventional integer-order cases.*

The following assumptions are needed for System (1).

Assumption 1. *The partial derivative of $f(\cdot,\cdot,\cdot,\cdot)$ is continuous for the control input $u(k)$.*

Assumption 2. *There exist positive constants u_M and y_M such that $|\Delta^a u(k)| \leq u_M$ and $|y(k)| \leq y_M$.*

Assumption 3. *For $\forall$ k, System (1) satisfies the Lipschitz condition*

$$|\Delta y(k+1)| \leq b|\Delta^a u(k)| \tag{4}$$

for $|\Delta^a u(k)| \neq 0$, where $\Delta y(k+1) = y(k+1) - y(k)$, $b > 0$ is a Lipschitz constant.

The objective of this paper is to design a data-driven robust FOMFAC law $u(k)$ for the nonlinear System (1) such that the tracking error $e(k) = y_d(k) - y(k)$ is uniformly bounded, with $y_d(k)$ as the desired trajectory.

By virtue of the third assumption, the nonlinear System (1) can be expressed by the following fractional-order dynamic data model [11]:

$$\Delta y(k+1) = \phi(k)\Delta^a u(k) \tag{5}$$

where $\phi(k)$ is a time-varying function. This function is called the fractional pseudo-partial derivative (FPPD), and satisfies $|\phi(k)| \leq b$. In this way, the robust FOMFAC law design problem is transformed into the design problem of $\Delta^a u(k)$.

3. Robust Fractional-Order Model-Free Adaptive Controller Design

3.1. PPD Parameter Estimation Algorithm

Because $\phi(k)$ in model (5) is unknown, a high-order estimation algorithm is needed to obtain the estimated value of $\hat{\phi}(k)$. Therefore, the following cost function for parameter estimation is used:

$$J(\phi(k)) = |\Delta y(k) - \phi(k)\Delta^a u(k-1)|^2 + \mu\Big|\phi(k) - \sum_{j=1}^{m} \alpha_j \hat{\phi}(k-j)\Big|^2 \tag{6}$$

where $m \in \mathbb{N}^+$ is the high-order degree, α_j are weighting coefficients with $\sum_{j=1}^{m} \alpha_j = 1$, and $\mu > 0$ is a penalty factor.

By calculating $\partial J(\phi(k))/\partial\phi(k) = 0$, the high-order PPD parameter estimation algorithm is expressed by

$$\hat{\phi}(k) = \frac{\Delta^a u(k-1)^2 \Delta y(k)}{\mu + |\Delta^a u(k-1)|^2} + \frac{\mu\eta \sum_{j=1}^{m} \alpha_j \hat{\phi}(k-j)}{\mu + |\Delta^a u(k-1)|^2}, \tag{7}$$

where η is the step-size factor [21].

Remark 2. *Compared with the first-order estimation algorithm [4–7], the parameter adaptive estimation law (7) is a high-order algorithm which can enhance the control performance by utilizing more historical data [8–10]. Although high-order algorithms imply more storage units and more computing complexity, there is a tradeoff between improved control performance and resource requirements.*

Remark 3. *At the first time, an initial value needs to be assigned to $\hat{\phi}(1)$. Because the calculation of $\hat{\phi}(k)$ relies on the previous m instances, it can only be computed when $k \geq m$. Therefore, the HOPPD parameter estimation algorithm (7) is only applied for $k \geq m$.*

Remark 4. *Here, $\boldsymbol{\alpha} = [\alpha_1, \alpha_2, \ldots, \alpha_m]$ represents the weights of the parameters estimated at the previous time. In general, these weights can be set as $\alpha_1 \geq \alpha_2 \geq \cdots \geq \alpha_m$.*

The stability of the sequence $\{\hat{\phi}(k)\}$ is stated in the following.

Remark 5. *In order to guarantee the well-posedness of the control scheme for all time instants, the following resetting algorithm is suggested:*

$$\hat{\phi}(k) = \hat{\phi}(1), \text{ if } \hat{\phi}(k) \leq \varepsilon \text{ or } \left|\Delta^a u(k-1)\right| \leq \varepsilon, \ \varepsilon > 0. \tag{8}$$

3.2. FOMFAC Law Design

The dynamic equation in terms of the tracking error $e(k) = y_d(k) - y(k)$ becomes

$$e(k+1) = e(k) - \phi(k)\Delta^a u(k) + \Delta y_d(k+1). \tag{9}$$

Consider the reference equation

$$e(k+1) = (1 - c_1)e(k), \tag{10}$$

where $c_1 \in (0, 2)$. From (9) and (10), the controller can be solved from

$$e(k) - \phi(k)\Delta^a u(k) + \Delta y_d(k+1) = (1 - c_1)e(k). \tag{11}$$

Therefore,

$$\Delta^a u(k) = \frac{1}{\phi(k)}\Big(c_1 e(k) - \Delta y_d(k+1)\Big). \tag{12}$$

Note that $\phi(k)$ is unknown and cannot be used directly. The inverse of $\phi(k)$ can be approximated by $\frac{\hat{\phi}(k)}{\lambda + \hat{\phi}^2(k)}$ for $\lambda > 0$, yielding the controller

$$\Delta^a u(k) = \frac{\hat{\phi}(k)}{\lambda + \hat{\phi}^2(k)}\Big(c_1 e(k) - \Delta y_d(k+1)\Big), \tag{13}$$

that is,

$$u(k) = \frac{\hat{\phi}(k)}{\lambda + \hat{\phi}^2(k)}\Big(c_1 e(k) - \Delta y_d(k+1)\Big) - \sum_{i=1}^{\min(k,N)} w(i,a)u(k-i). \tag{14}$$

Summarizing, the HOPPD-based FOMFAC algorithm is provided by (15).

$$\begin{cases} \hat{\phi}(k) = \hat{\phi}(k-1) + \frac{\eta \Delta^a u(k-1)[\Delta y(k) - \hat{\phi}(k-1)\Delta^a u(k-1)]}{\mu + |\Delta^a u(k-1)|^2}, & 2 \le k < m \\ \hat{\phi}(k) = \frac{\Delta^a u(k-1)\Delta y(k)}{\mu + |\Delta^a u(k-1)|^2} + \frac{\mu\eta \sum_{j=1}^{m} \alpha_j \hat{\phi}(k-j)}{\mu + |\Delta^a u(k-1)|^2}, & k \ge m \\ \hat{\phi}(k) = \hat{\phi}(1), \text{if } \hat{\phi}(k) \le \varepsilon \text{ or } \left|\Delta^a u(k-1)\right| \le \varepsilon, \ \ \varepsilon > 0, \\ u(k) = \frac{\hat{\phi}(k)}{\lambda + \hat{\phi}^2(k)}\Big(c_1 e(k) - \Delta y_d(k+1)\Big) - \sum_{i=1}^{\min(k,N)} w(i,a)u(k-i) \end{cases} \tag{15}$$

Remark 6. *In comparison with the existing FOMFAC law in [11,12], our novel controller incorporates more historical input and output data, enriching the gain parameters by involving $\hat{\phi}(k)$ due to the inclusion of fractional-order and high-order algorithms.*

Remark 7. *In the HOPPD-based FOMFAC algorithm provided in (15), larger values of λ and μ mean a faster convergence; however, overshooting may occur as a tradeoff, while smaller values of η indicate faster convergence [10]. In addition, if the control knowledge is close to the current iteration, its weight coefficient may be large, and vice versa; therefore, it is generally possible to select $\alpha_1 \ge \alpha_2 \ge \cdots \ge \alpha_m$ for the algorithm of order m. The HOPPD-based FOMFAC algorithm (15) contains some parameters that affect the control performance. It can be optimized, for instance by using particle swarm optimization, which is a significant topic for future research.*

3.3. Robust Stability Analysis

In many industrial environments, the system output is can be contaminated by measurement disturbances. Therefore, the measurement output can be rewritten as

$$y_o(k) = y(k) + \omega(k), \tag{16}$$

where $y_o(k)$ is the measurement output and $\omega(k)$ is the measurement disturbance. In this case, the corresponding HOPPD-based RFOMFAC algorithm is described as follows:

$$\begin{cases} \hat{\phi}(k) = \hat{\phi}(k-1) + \frac{\eta \Delta^a u(k-1)[\Delta y_o(k) - \hat{\phi}(k-1)\Delta^a u(k-1)]}{\mu + |\Delta^a u(k-1)|^2}, & 2 \le k < m \\ \hat{\phi}(k) = \frac{\Delta^a u(k-1)\Delta y_o(k)}{\mu + |\Delta^a u(k-1)|^2} + \frac{\mu\eta \sum_{j=1}^{m} \alpha_j \hat{\phi}(k-j)}{\mu + |\Delta^a u(k-1)|^2}, & k \ge m \\ \hat{\phi}(k) = \hat{\phi}(1), \text{if } \hat{\phi}(k) \le \varepsilon \text{ or } \left|\Delta^a u(k-1)\right| \le \varepsilon, \ \ \varepsilon > 0, \\ u(k) = \frac{\hat{\phi}(k)}{\lambda + \hat{\phi}^2(k)}\Big(c_1(y_d(k) - y_o(k)) - \Delta y_d(k+1)\Big) - \sum_{i=1}^{\min(k,N)} w(i,a)u(k-i). \end{cases} \tag{17}$$

The following lemma is developed first.

Lemma 1. *For the nonlinear System (5), if Assumptions 1–3 hold, then $\hat{\phi}(k)$ in (17) is uniformly ultimately bounded $\forall$ k with $\mu > 0$, $\eta \in (0, 1]$, and $\sum_{j=1}^{m} \alpha_j = 1$.*

Proof. When $2 \leq k < m$,

$$\hat{\phi}(k) = \left(1 - \eta \frac{|\Delta^a u(k-1)|^2}{\mu + |\Delta^a u(k-1)|^2}\right)\hat{\phi}(k-1) + \eta \frac{\Delta^a u(k-1)\Delta y_o(k)}{\mu + |\Delta^a u(k-1)|^2}. \tag{18}$$

From the assumptions on System (1), we have

$$-\infty < \eta\left(\frac{\Delta^a u(k-1)\Delta y_o(k)}{\mu + |\Delta^a u(k-1)|^2}\right) < \infty, \tag{19}$$

whenever $|\Delta^a u(k-1)\Delta y_o(k)| < \infty$ since $0 < \mu < \mu + |\Delta^a u(k-1)|^2$. According to Assumptions 2 and 3, we have

$$|\Delta^a u(k-1)\Delta y_o(k)| \leq (b + 2b_w)|\Delta^a u(k-1)|^2. \tag{20}$$

Consequently,

$$\left|\frac{\Delta^a u(k-1)\Delta y_o(k)}{\mu + |\Delta^a u(k-1)|^2}\right| \leq \frac{b|\Delta^a u(k-1)|^2}{\mu + |\Delta^a u(k-1)|^2} \leq (b + 2b_w) < \infty. \tag{21}$$

If we choose $\mu > 0$, $\eta \in (0, 1]$, then

$$\eta \Delta^a u^2(k-1)^2 < \Delta^a u^2(k-1) < \mu + \Delta^a u^2(k-1), \tag{22}$$

which leads to

$$0 \leq \left|1 - \eta \frac{|\Delta^a u(k-1)|^2}{\mu + |\Delta^a u(k-1)|^2}\right| < 1. \tag{23}$$

From (18), (21), and (23), we can conclude that $\hat{\phi}(k)$ is uniformly ultimately bounded.

When $k \geq m$, by taking the absolute value on both sides, we obtain from $\hat{\phi}(k)$ in (17) that

$$\begin{aligned} |\hat{\phi}(k)| &\leq \left|\frac{\Delta^a u(k-1)\Delta y_o(k)}{\mu + |\Delta^a u(k-1)|^2}\right| + \left|\frac{\mu\eta \sum_{j=1}^{m} \alpha_j \hat{\phi}(k-j)}{\mu + |\Delta^a u(k-1)|^2}\right| && (24) \\ &\leq (b + 2b_w) + \eta\left|1 - \frac{|\Delta^a u(k-1)|^2}{\mu + |\Delta^a u(k-1)|^2}\right|\left|\sum_{j=1}^{m} \alpha_j \hat{\phi}(k-j)\right| \\ &\leq (b + 2b_w) + \eta\left|\sum_{j=1}^{m} \alpha_j \hat{\phi}(k-j)\right|. && (25) \end{aligned}$$

As the boundedness of $\sum_{j=1}^{m} \alpha_j \hat{\phi}(k-j)$ has already been demonstrated, $\hat{\phi}(k)$ is uniformly ultimately bounded and the proof is completed. □

Theorem 1. *For the nonlinear System (1) with Assumptions 1–3 and using the HOPPD-based FOMFAC algorithm (17), if $\mu > 0$, $\eta \in (0, 1]$, and $\lambda > \frac{c_1^2 b^2}{4}$, then the tracking error $e(k)$ is uniformly ultimately bounded.*

Proof. We define the measurement error $e_o(k) = y_d(k) - y_o(k)$. From (5), (13), and (16), we have

$$\Delta^a u(k) = \frac{c_1 \hat{\phi}(k)}{\lambda + \hat{\phi}^2(k)} e_o(k) = \frac{c_1 \hat{\phi}(k)}{\lambda + \hat{\phi}^2(k)}(e(k) - \omega(k)). \tag{26}$$

Substituting the control input (26) into (9), we have

$$e(k+1) = \Big[1 - \frac{c_1\phi(k)\hat{\phi}(k)}{\lambda + \hat{\phi}^2(k)}\Big]e(k) + \frac{c_1\phi(k)\hat{\phi}(k)}{\lambda + \hat{\phi}^2(k)}\omega(k). \tag{27}$$

Because $\lambda > \frac{c_1^2 b^2}{4} \geq \frac{c_1^2\phi^2(k)}{4}$, we have

$$0 < d_1 \leq \frac{c_1\phi(k)\hat{\phi}(k)}{\lambda + \hat{\phi}^2(k)} \leq d_2 < 1. \tag{28}$$

Thus, (27) yields

$$\begin{aligned} |e(k+1)| &\leq (1-d_1)|e(k)| + d_2 b_w \\ &\leq (1-d_1)^2|e(k-1)| + (1-d_1)d_2 b_w + d_2 b_w \\ &\leq (1-d_1)^k|e(1)| + (1-d_1)^{k-1}|d_2 b_w \\ &+ \cdots + (1-d_1)d_2 b_w + d_2 b_w, \end{aligned} \tag{29}$$

which implies that

$$\lim_{k\to\infty}|e(k)| \leq \frac{d_2 b_w}{d_1} < \frac{b_w}{d_1}. \tag{30}$$

The proof is completed. □

3.4. FOMFAC with Variable Gain

The modified FOMFAC algorithm with variable gain is constructed as follows:

$$\Delta^a u(k) = \frac{c_1\hat{\phi}(k)}{\lambda + \hat{\phi}^2(k)}\frac{(y_d(k) - y_o(k))}{k+1}. \tag{31}$$

Theorem 2. *For the nonlinear System* (1) *under the FOMFAC law* (31)*, if the conditions in Theorem 1 are satisfied, then the tracking error* $e(k)$ *satisfies* $\lim_{k\to\infty} e(k) = 0$.

Proof. From (5), (13), and (31), we have

$$\Delta^a u(k) = \frac{c_1\hat{\phi}(k)}{\lambda + \hat{\phi}^2(k)}\Big(\frac{e(k)}{k+1} - \frac{\omega(k)}{k+1}\Big). \tag{32}$$

Substituting the control input (31) into (9), we have

$$e(k+1) = \Big[1 - \frac{c_1\phi(k)\hat{\phi}(k)}{(\lambda + \hat{\phi}^2(k))(k+1)}\Big]e(k) + \frac{c_1\phi(k)\hat{\phi}(k)}{(\lambda + \hat{\phi}^2(k))(k+1)}\omega(k). \tag{33}$$

Because

$$0 < d_1 \leq \frac{c_1\phi(k)\hat{\phi}(k)}{\lambda + \hat{\phi}^2(k)} = \theta(k) \leq d_2 < 1, \tag{34}$$

from (33) we have

$$\begin{aligned}
|e(k+1)| &\leq \Big(1-\frac{d_1}{k+1}\Big)|e(k)|+\frac{d_2}{k+1}b_w \\
&\leq \Big(1-\frac{d_1}{k+1}\Big)\Big(1-\frac{d_1}{k}\Big)|e(k-1)|+\Big(1-\frac{d_1}{k+1}\Big)\frac{d_2}{k}b_w+\frac{d_2b_w}{k+1} \\
&\leq \Big(1-\frac{d_1}{k+1}\Big)\Big(1-\frac{d_1}{k}\Big)\cdots(1-d_1)|e(0)|+\Big[\Big(1-\frac{d_1}{k+1}\Big)\Big(1-\frac{d_1}{k}\Big)\cdots\Big(1-\frac{d_1}{2}\Big) \\
&+ \cdots+\Big(1-\frac{d_1}{k+1}\Big)\Big(1-\frac{d_1}{k}\Big)\frac{1}{k-1}+\Big(1-\frac{d_1}{k+1}\Big)\frac{1}{k}+\frac{1}{k+1}\Big]d_2b_w.
\end{aligned} \tag{35}$$

Clearly, there exists a positive constant ξ such that

$$0<\xi\leq\frac{d_1}{k+1}<\frac{d_1}{k}<\cdots<d_1<1 \tag{36}$$

and

$$1-d_1<\cdots<1-\frac{d_1}{k}<1-\frac{d_1}{k+1}\leq 1-\xi<1. \tag{37}$$

It follows from (35) and (37) that

$$|e(k+1)| \leq (1-\xi)^{k+1}|e(0)|+\Big[(1-\xi)^k+\frac{1}{2}(1-\xi)^{k-1}+\cdots+\frac{1}{k}(1-\xi)+\frac{1}{k+1}\Big]d_2b_w. \tag{38}$$

For given k, if k is even, then

$$\begin{aligned}
|e(k+1)| &\leq (1-\xi)^{k+1}|e(0)|+d_2b_w\Big[(1-\xi)^k+\frac{1}{2}(1-\xi)^{k-1} \\
&+ \cdots+\frac{1}{(k/2)}(1-\xi)^{(k/2)+1} \\
&+ \frac{1}{(k/2)+1}(1-\xi)^{(k/2)}+\cdots+\frac{1}{k}(1-\xi)+\frac{1}{k+1}\Big] \\
&\leq (1-\xi)^{(k/2)}|e(0)|+d_2b_w(1-\xi)^{(k/2)}\Big(1+\frac{1}{2}+\cdots+\frac{1}{k/2}\Big) \\
&+ d_2b_w\frac{1}{(k/2)+1}\Big[(1-\xi)^{(k/2)}+\cdots+(1-\xi)+1\Big] \\
&\leq (1-\xi)^{(k/2)}\Big(|e(0)|+\frac{k}{2}d_2b_w\Big)+d_2b_w\frac{1}{(k/2)+1}\cdot\frac{1}{\xi},
\end{aligned} \tag{39}$$

which implies that $\lim\limits_{k\to\infty}|e(k)|=0$.

Similarly, if k is odd, then we have

$$\begin{aligned}
|e(k+1)| &\leq (1-\xi)^{k+1}|e(0)|+d_2b_w\Big[(1-\xi)^k+\frac{1}{2}(1-\xi)^{k-1} \\
&+ \cdots+\frac{1}{(k+1)/2}(1-\xi)^{(k+1)/2}+\frac{1}{((k+1)/2)+1}(1-\xi)^{((k+1)/2)-1} \\
&+ \cdots+\frac{1}{k}(1-\xi)+\frac{1}{k+1}\Big] \\
&\leq (1-\xi)^{(k+1)/2}|e(0)|+d_2b_w(1-\xi)^{(k+1)/2}\Big(1+\frac{1}{2}+\cdots+\frac{1}{(k+1)/2}\Big) \\
&+ d_2b_w\frac{1}{((k+1)/2)+1}\Big[(1-\xi)^{((k+1)/2)-1}+\cdots+(1-\xi)+1\Big] \\
&\leq (1-\xi)^{(k+1)/2}\Big(|e(0)|+\frac{k+1}{2}d_2b_w\Big)+d_2b_w\frac{1}{((k+1)/2))+1}\cdot\frac{1}{\xi},
\end{aligned} \tag{40}$$

which also implies that $\lim_{k\to\infty} |e(k)| = 0$. The proof is completed. □

4. Application to Speed Control of DC Motor System

In this section, we apply the proposed RFOMFAC algorithm to the speed control of a DC motor system, which we selected from [22] to validate the effectiveness of our algorithm.

Example 1. *The schematic diagram of the DC motor is illustrated in Figure 1. The dynamics of the DC motor are as follows:*

$$u_a = L_a \frac{di_a}{dt} + i_a R_a + E_a \tag{41}$$

$$J \frac{\omega_m(t)}{dt} = T_e - T_L \tag{42}$$

where u_a, i_a, R_a, and L_a are the voltage, current, resistance, and inductance of the armature, respectively, $E_a = C_e\omega_m(t)$ represents the potential of the armature, $T_e = C_e i_a$, C_e, ω_m, and T_L represent the torque, coefficient of potential, rotation speed, and load torque, respectively, and J stands for the total value of the moment of the inertia converted into the motor axis. The relevant parameters are set as $L_a = 0.01\ H$, $R_a = 1.20\ \Omega$, $C_e = 0.3\ Nm/A^2$, $J = 0.208\ kg{\cdot}m^2$, and $T_L = 18\ Nm$.

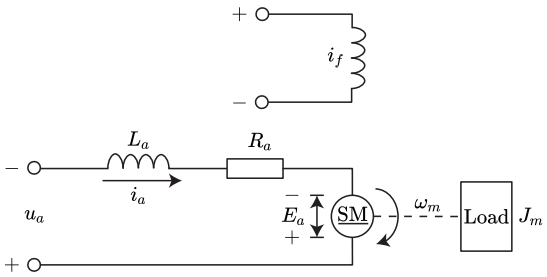


Figure 1. Schematic diagram of the DC motor.

The transfer function of the DC motor speed relative to the input voltage is [22]

$$H(s) = \frac{\omega_m(s)}{u_a(s)} = \frac{1.6338}{0.00650s^2 + 0.3023s + 1}. \tag{43}$$

Therefore, the difference equation of the DC motor is

$$y(k+1) = 0.3902u(k) + 0.09525u(k-1) + 0.7125y(k) - 0.009554y(k-1), \tag{44}$$

where $y(k)$ and $u(k)$ are the DC motor speed and the input voltage, respectively.

The reference DC motor speed is

$$y_d(k) = \begin{cases} 1, & 0 < k \le 40, \\ 2 & 40 < k \le 80, \\ 1.5, & 80 < k \le 120. \end{cases} \tag{45}$$

The initial conditions are $u(-1) = u(0) = 0$, $y(-1) = y(0) = -0.20$, and $\varepsilon = 10^{-5}$, while the controller parameters are $\lambda = 0.2$, $\rho = 0.1$, $\mu = 0.02$, $c_1 = 0.8$, and $\eta = 0.7$. The predefined number is fixed at $L = 100$. The fractional order is set as $n = 0.8$. The high-order estimation is configured with $m = 3$, and the weighting coefficients are $\alpha_1 = 0.45$, $\alpha_2 = 0.45$, and $\alpha_3 = 0.1$. The high-order estimation algorithm commences at $k = 4$. The initial PPD is uniformly set as $\hat{\phi}(1) = 2$ for all controllers.

The simulation results are shown in Figure 2. The results illustrate the tracking performance of different controllers in response to the given reference signal for the ideal case ($\omega(k) = 0$). It can be seen that the system output has bounded stability. Compared with the traditional FOMFAC method [19], the proposed HOPPD-based RFOMFAC algorithm has a faster response speed.

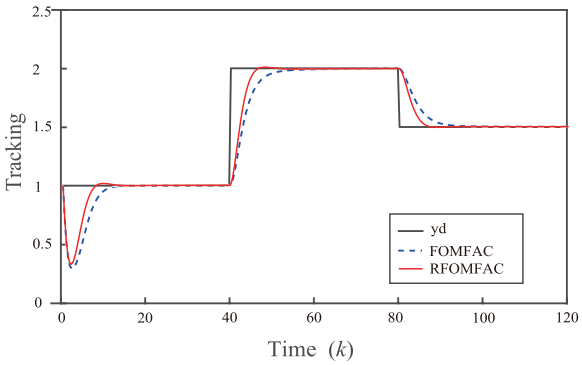


Figure 2. System output under different controllers.

To test the robustness of the proposed HOPPD-based RFOMFAC algorithm, the measurement disturbance $\omega(k) = 0.1*\text{rand}(1, 10)$ was added. The resulting system contains changes in the desired output. The tracking performance results are shown in Figures 3 and 4. In the proposed HOPPD-based RFOMFAC algorithm, the parameter estimation response curves of the PPD are displayed in Figure 5. It can be observed that the PPD estimator adjusts the estimation values under different situations. Figure 6 shows the control input.

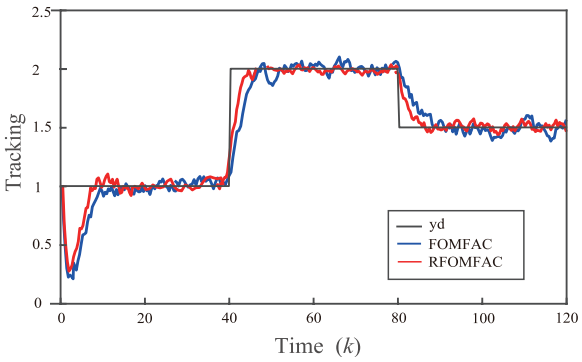


Figure 3. System output under different controllers with measurement disturbance.

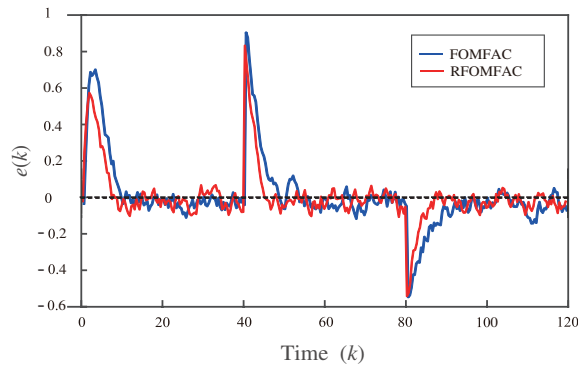


Figure 4. Tracking error with measurement disturbance.

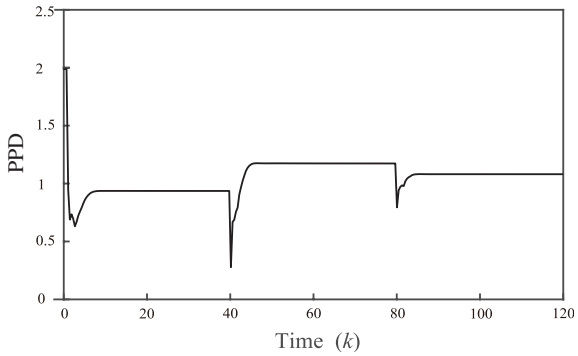


Figure 5. Parameter estimation response of PPD.

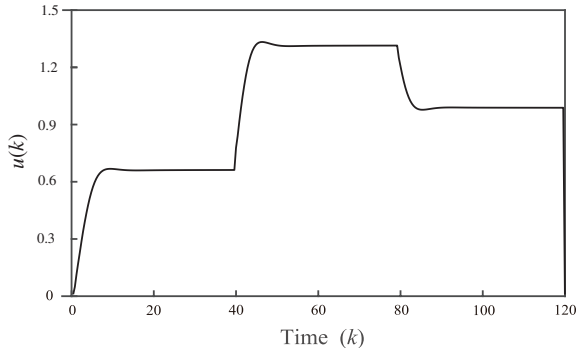


Figure 6. Control input $u(k)$.

Table 1 presents the comparison results of the sum square error (SSE) and sum square control (SSC) for the different controllers. It can be observed that the system outputs possess bounded stability even under the effect of measurement disturbance. However, better system control performance can be obtained under the proposed HOPPD-based RFOMFAC algorithm, which shortens the response time and reduces the tracking error.

Table 1. Comparison of SSE and SSC with different controllers.

CONTROLLER	SSE	SSC
FOMFAC [11]	31.3524	1.8514
RFOMFAC	30.5291	1.3573

5. Conclusions

This paper considers a HOPPD-based RFOMFAC algorithm for a class of uncertain discrete-time nonlinear systems. A fractional-order dynamic data model is used to express the discrete-time nonlinear systems, then a high-order estimation algorithm is applied to obtain the estimated PPD value. By considering the desired reference equation and the HOPPD-based RFOMFAC law, a robust stability analysis can be presented. Furthermore, to account for outputs with measurement disturbances, a modified RFOMFAC algorithm with variable gain is constructed to investigate the influence of such disturbances. Results demonstrate that the robust stability of the algorithm can be guaranteed. We applied our proposed RFOMFAC algorithm to the speed control of a DC motor system in order to validate its effectiveness. It is worth noting that the parameters of the controller can be optimized to accomplish specific real objectives or to achieve further experimental results, which are the objects of our future research work.

Author Contributions: Conceptualization and methodology, H.W.; software, H.J.; formal analysis, J.H.; writing and editing, Y.L. All authors have read and agreed to the published version of the manuscript.

Funding: This study was supported by Natural Science Foundation of Hunan Province (2022JJ60057) and the Science and Technology Project of Jiangxi Educational Bureau (GJJ2202208).

Data Availability Statement: Data are contained within the article.

Conflicts of Interest: The authors declare no conflicts of interest.

References

1. Hou, Z.S.; Xu, J.X. On data-driven control theory: The state of the art and perspective. *Acta Autom. Sin.* **2009**, *35*, 650–667. [CrossRef]
2. Yue, B.F.; Su, M.Y.; Jin, X.Z.; Che, W.W. Event-triggered MFAC of nonlinear NCSs against sensor faults and DoS attacks. *IEEE Trans. Circuits Syst. II Express Briefs* **2022**, *69*, 4409–4413. [CrossRef]
3. Zhao, C.; Xie, Z.; Zhou, F. Model-free adaptive control for wind power system based on grey prediction under unbalanced grid conditions. *Electr. Power Syst. Res.* **2023**, *225*, 109809. [CrossRef]
4. Wang, Y.; Shen, C.; Huang, J.; Chen, H. Model-free adaptive control for unmanned surface vessels: A literature review. *Syst. Sci. Control Eng.* **2024**, *12*, 2316170. [CrossRef]
5. Song, W.; Feng, J.; Liu, J. Distributed MIMO MFAC-based consensus tracking strategy for multiagent systems with fixed and switching topologies. *Int. J. Syst. Sci.* **2022**, *53*, 1888–1905. [CrossRef]
6. Pham, H.A.; Soffker, D. Improved model-free adaptive predictive control based on recursive least-squares estimation algorithm. *Asian J. Control* **2023**, *25*, 1745–1758. [CrossRef]
7. Heydari, M.; Darvishpoor, S.; Novinzadeh, A.B.; Roshanian, J. On the performance of the model-free adaptive control for a novel moving-mass controlled flying robot. *J. Intell. Robot. Syst.* **2024**, *110*, 79. [CrossRef]
8. Ai, Q.; Ke, D.; Zuo, J.; Meng, W.; Liu, Q.; Zhang, Z.; Xie, S.Q. High-order model-free adaptive iterative learning control of pneumatic artificial muscle with enhanced convergence. *IEEE Trans. Ind. Electron.* **2019**, *67*, 9548–9559. [CrossRef]
9. Wang, Z.; Gao, F.; Liu, F. Improved high order model-free adaptive iterative learning control with disturbance compensation and enhanced convergence. *CMES-Comput. Model. Eng. Sci.* **2023**, *124*, 344–355. [CrossRef]
10. Xu, J.; Lin, N.; Chi, R.; Li, X. High-order model-free adaptive iterative learning control. *Trans. Inst. Meas. Control* **2023**, *45*, 1886–1895. [CrossRef]
11. Aldo, J.; Chidentree, T. Fractional data-driven model for stabilization of uncertain discrete-time nonlinear systems. *J. Frankl. Inst.* **2022**, *359*, 9690–9702.
12. Chidentree, T.; Aldo, J. Model-free adaptive control based on fractional input-output data model. *Appl. Sci.* **2022**, *12*, 11168. [CrossRef]
13. Zhang, W.; Xu, D.; Jiang, B.; Shi, P. Event-triggered model-free adaptive fractional order sliding mode I/O constrained control for a class of nonlinear systems. *Int. J. Robust Nonlinear Control* **2023**, *33*, 10151–10174. [CrossRef]
14. Veisi, A.; Delavari, H. Fractional data driven controller based on adaptive neural network optimizer. *Expert Syst. Appl.* **2024**, *257*, 125077. [CrossRef]
15. Lan, Y.H.; Zhao, J.Y. Improving track performance by combining Padé-approximation-based preview repetitive control and equivalent-input-disturbance. *J. Electr. Eng. Technol.* **2024**, *1*, 3781–3794. [CrossRef]
16. Liu, S.; Hou, Z.; Zhang, X.; Ji, H. Model-free adaptive control method for a class of unknown MIMO systems with measurement noise and application to quadrotor aircraft. *IET Control Theory Appl.* **2020**, *14*, 2084–2096. [CrossRef]
17. Ren, C.; Zhang, J.; Li, W.; Ma, S. Data-driven model free adaptive control for an omnidirectional mobile manipulator using neural network. In Proceedings of the 2020 IEEE/ASME International Conference on Advanced Intelligent Mechatronics, Boston, MA, USA, 6–9 July 2020; pp. 1002–1007.
18. Yu, W.; Wang, R.; Bu, X.; Hou, Z. Model free adaptive control for a class of nonlinear systems with fading measurements. *J. Frankl. Inst.* **2020**, *357*, 7743–7760. [CrossRef]
19. Corradini, M.L. A robust sliding-mode based data-driven model-free adaptive controller. *IEEE Control Syst. Lett.* **2021**, *6*, 421–427. [CrossRef]
20. Wang, C.; Huo, X.; Ma, K.; Ji, R. PID-like model free adaptive control with discrete extended state observer and its application on an unmanned helicopter. *IEEE Trans. Ind. Inform.* **2023**, *19*, 11265–11274. [CrossRef]

21. Lv, Z.-X.; Liao, J. Fractional-order model-free adaptive control with high order estimation. *Mathematics* **2024**, *12*, 784. [CrossRef]
22. Jin, X.; Ma, Y.; Che, W. An improved model-free adaptive control for nonlinear systems: An LMI approach. *Appl. Math. Comput.* **2023**, *447*, 127910. [CrossRef]

Disclaimer/Publisher's Note: The statements, opinions and data contained in all publications are solely those of the individual author(s) and contributor(s) and not of MDPI and/or the editor(s). MDPI and/or the editor(s) disclaim responsibility for any injury to people or property resulting from any ideas, methods, instructions or products referred to in the content.